Polarization resolved measurement of Rayleigh backscatter in fiber-optic components

B. J. Soller, M. Wolfe, M. E. Froggatt
Luna Technologies, 3157 State Street, Blacksburg, VA 24060
sollerb@lunatechnologies.com

1. Introduction

Fiber-optic components, modules and assemblies for modern networking applications are becoming more complex. At the component and module level, failures such as bad splices, bends, crimps, and other non-reflective events can be extremely difficult to locate and troubleshoot. The available measurement techniques designed to identify these types of failures fall into two basic categories: optical time domain reflectometry (OTDR), and frequency domain reflectometry. Typically, OTDRs lack sufficient spatial resolution to be useful at the component and module level where one might be interested in, say, locating a bad splice in a concatenation of a dozen WDM components.

Optical frequency domain reflectometry (OFDR) is a tunable laser-based frequency domain technique that has several distinct advantages over time domain and low coherence techniques when the optical systems under consideration are several tens of meters in length [1,2]. Specifically, OFDR has advantages in that it is capable of sub-millimeter resolution measurements over multiple tens of meters of optical length with high sensitivity and dynamic range.

In this paper, we introduce a method for fiber-optic testing and troubleshooting at the assembly level that is based on using OFDR to measure the distributed Rayleigh backscatter along the length of the fiber-optic network. Rayleigh scattering in optical fiber is caused by material density and radius fluctuations along the length of the core. Measuring the distribution of the light scattered in the backward direction as a function of length down a fiber-optic assembly can be useful in identifying breaks, bad spices and non-reflective events. Rayleigh scatter can also be used to measure distributed loss and gain [3], induced stress and strain [4], temperature [5], and local birefringence [6]. We report polarization resolved measurement of the distributed reflections in an optical system with -130 dB sensitivity and 60 dB dynamic range with 40 μm resolution over 30 meters of optical length. The applications presented show that the system can be used to quantitatively measure both insertion and return loss with accuracy and resolution on the order of 0.1 dB. We also show that the system can be used to track changes in the state of polarization (SOP) of the probe light as it propagates through the network. This method has significant advantages in range, resolution, speed and usability when compared to conventional reflectometers.

2. Experiment

The optical network used to measure polarization resolved Rayleigh backscatter is shown in Fig. 1. Light from a tunable laser source is split into measurement and reference optical paths. In the measurement path, the light is further split by a 50/50 coupler. A third coupler is used to recombine the light from the measurement path with the light from the reference path. After recombination, the light is split by a polarization beam splitter. Interference is detected at two PIN photodiodes that are connected via amplification circuitry to a 12-bit, 5 mega-samples per second National Instruments data acquisition card (DAQ).

The laser source is a commercially available continuously tunable external cavity laser diode. The typical tuning range is from 2.5 nm to 40 nm centered at 1550 nm with a tuning rate of 20 nm/s. The laser is controlled via analog voltage ramp from the DAQ card. The line-width of the laser is 200 kHz.

Not shown in the figure is an auxiliary interferometer used to monitor phase error during laser tuning. This technique is called triggered acquisition and is common in OFDR systems to remove laser tuning errors from the data [1]. Also not shown is a portion of the network wherein a HCN gas-cell is used to monitor the instantaneous wavelength of the scanning laser. Hence, for a given scan data is being taken across the DAQ on four channels simultaneously.

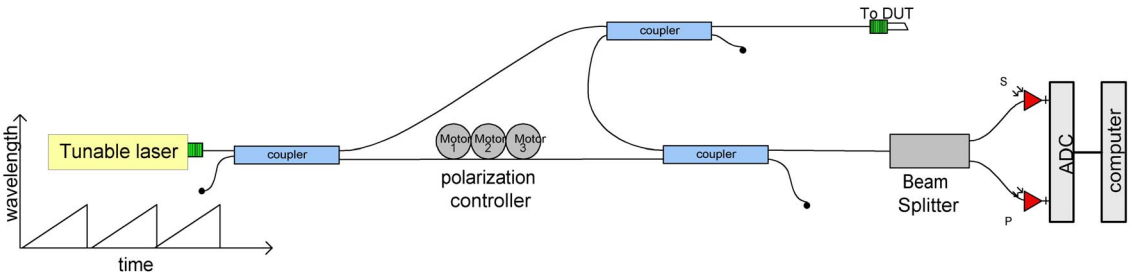

Fig. 1. Optical network used to perform polarization diverse measurements of Rayleigh backscatter. The couplers are all 50/50 and the ADC represents a high-speed digital data acquisition card (12 bit, 5 mega-samples per second).

The maximum measurable length for this instrument is determined by the sampling resolution in the frequency domain which is in turn determined by the physical delay difference of the auxiliary interferometer used for data triggering. In this case the delay in the auxiliary interferometer was 800 ns. Dividing this number by 2 twice, once for Nyquist and once because of the double-pass nature of the measurement interferometer, gives us a maximum measurable delay difference of 200 ns, or a maximum length differential of 40 m in fiber.

Of course a longer differential delay in the auxiliary interferometer would result in access to more length in the measurement arm. This raises a central difficulty. The bandwidth in the acquisition and amplification electronics must be carefully chosen so as to eliminate as much noise from the measurement as possible. Measurement of longer lengths requires greater bandwidth which raises the noise levels in the system beyond the Rayleigh level.

3. Interference and polarization effects

Consider a reflection within the device under test (DUT) with a time-of-flight delay differential with the reference path of 'τ'. For a laser sweep described by the instantaneous frequency $\omega(t) = \omega_o + \gamma t + \sigma(t)$ where γ is the tuning rate and $\sigma(t)$ is the (small) tuning error, interference signals at the detectors labeled 's' and 'p' in Fig. 1 for this reflection will be of the form

$$E_s(t) = 2r_\tau g_s(\tau)\left[(\hat{T}_s\vec{E}_{meas})\cdot(\hat{T}_s\vec{E}_{ref})\right]\cos\left(\omega_o\tau + \gamma\tau t + \sigma(t-\tau)\tau + \phi_\tau\right), \quad (1)$$

$$E_p(t) = 2r_\tau g_p(\tau)\left[(\hat{T}_p\vec{E}_{meas})\cdot(\hat{T}_p\vec{E}_{ref})\right]\cos\left(\omega_o\tau + \gamma\tau t + \sigma(t-\tau)\tau + \phi_\tau\right), \quad (2)$$

where r_τ and ϕ_τ are the amplitude and phase of the complex reflectivity of the event, $\vec{E}_{meas}$ is the vector electric field amplitude from the measurement path at the beam splitter, $\vec{E}_{ref}$ is the vector amplitude from the field in the reference arm, $\hat{T}_s$ and $\hat{T}_p$ are projection operators that represent the orthogonal states of the beam splitter [7] and $g_s(\tau)$ and $g_p(\tau)$ are the frequency dependent gains of the two data acquisition channels.

Equations (1) and (2) clearly illustrate the polarization sensitivity of the OFDR technique. In the absence of the beam splitter and two-channel acquisition, the interference amplitude is a function of the relative alignment of the reference and measurement fields. The polarization controller in the reference arm of the network combined with the polarization beam splitter allows the reference field to be aligned such that it is split evenly between the two states 's' and 'p' of the beam splitter. This ensures that an interference signal will be present on at least one of the detectors irrespective of the polarization state of the field reflected from the DUT; a condition not necessarily met in the absence of the beam splitter. This is of particular importance for the results described here, because for a given launch state in the measurement arm, small amounts of birefringence along the length of the DUT cause the polarization state of the reflected signal to be completely undetermined.

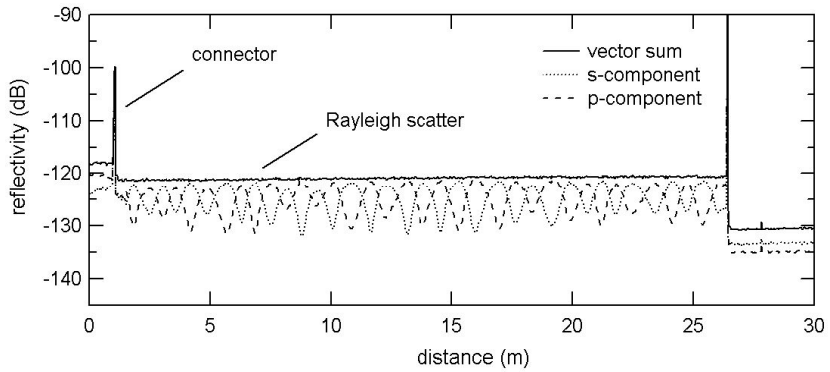

Fig. 2. The reflectivity of a 25 meter spool (2 in radius) of standard single-mode fiber. The solid curve is the vector sum of the two dashed curves. The dashed curves are the amplitude of the Fourier transform of the interference signals measured on the two detectors shown in Fig. 1 labeled 's' and 'p'. The oscillations in the dashed curves are caused by birefringence (or PMD) induced in the fiber due to the wind.

The equations above that describe the interference are written as a function of time, '*t*'. This is the "lab" time and reflects the fact that the tunable laser is scanned as a function of time, $\omega = \omega(t)$. So, Eqs. (1) and (2) are a frequency domain description of the DUT. By transforming these equations to the time domain, we can build a representation of the reflections in a device or assembly under test as a function of length. This is accomplished by a Fourier transform of the frequency domain results into the time domain.

Figure 2 shows time domain results for a 25 meter spool of fiber. The laser scan was from 1535 nm to 1575 nm which corresponds to a bandwidth of 5 THz. The spatial resolution of in the data is dictated by the scan bandwidth according to $\Delta z = c/2n_g\Delta f$ where n_g is the group delay of material under test, c is the speed of light and Δf is the bandwidth of the measurement scan. For this scan this comes to 20 μm. In reality, small amounts of residual dispersion, laser tuning errors and other environmental effects combine to result in a two-point resolution of closer to 40 μm. Scanning at 20 nm/s, the total measurement time including processing for this data set is approximately 3.5 seconds. No averaging was performed to achieve this data, however the data displayed in Fig. 2 was filtered with an effective bandwidth of approximately 10 mm.

The two dashed curves represent the amplitude of the Fourier transform of the signals on the s- and p-detectors. If the Fourier transform of the frequency domain signals $E_s(t)$ and $E_p(t)$ (remembering that these are functions of frequency, $\omega = \omega(t)$, and '*t*' is in the lab frame) then the transforms can be written: $\tilde{E}_s(\tau)$ and $\tilde{E}_p(\tau)$. The total reflectivity in the time domain is given by the vector sum

$$r(\tau) = \sqrt{\left|\tilde{E}_s(\tau)\right|^2 + \left|\tilde{E}_p(\tau)\right|^2} \quad . \tag{3}$$

The solid curve in Fig. 2 is the vector sum of the two Fourier transformed signals $\tilde{E}_s(\tau)$ and $\tilde{E}_p(\tau)$. Note that performing this operation in the time domain as opposed to the frequency domain is advantageous in that one avoids the non-linear operation of summing and squaring sinusoidally varying signals.

The absolute referencing of the reflectivity axis is accomplished by measuring the response of a nearly perfectly reflecting gold plated polished fiber tip. In doing this, one must confirm that the amplifier response is linear over the entire range of the system (130 dB).

4. Results and discussion

The distributed reflectivity of the fiber shown in Fig. 2 at -120 dB is due to the Rayleigh backscatter. The figure also shows the noise floor of the system (beyond 26.5 m) at about -130 dB. Excluding the loss in the first connector, this gives a 13 dB overhead from the scatter level to the noise floor. With a carefully calibrated system, this dynamic range allows one to monitor the level of Rayleigh scatter to determine certain metrics of the DUT. Specifically, insertion loss and return loss events can be located spatially with high resolution, and their values can be measured quantitatively.

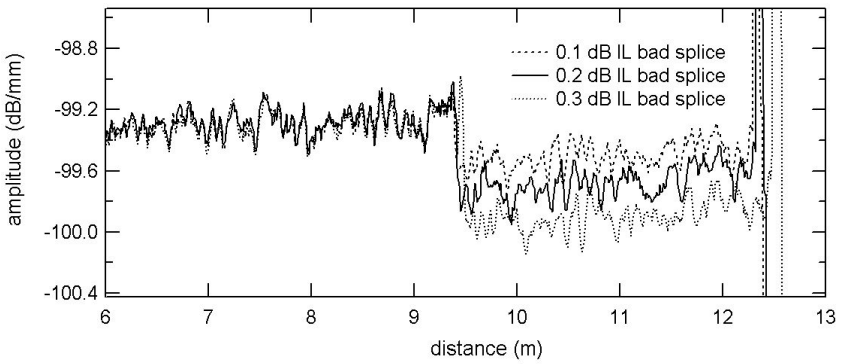

Fig. 3. Rayleigh backscatter measured through three known bad splices in SMF-28. Because the backscatter experiences the loss twice, a 0.1 dB loss is recorded as a 0.2 dB drop in the backscatter level. The same length of fiber was used leading up to each splice. Note the repeatability in the scatter signature from the fiber leading up to the splices.

Figure 3 displays the results of a measurement of the backscatter through three known bad splices. The backscatter level can be integrated on either side of the splice and compared in order to get a measure of the splice's insertion loss. In this case, the insertion loss resolution is on the order of 0.05 dB, as all three bad splices are clearly identifiable. Because the reflected waves experience the loss of an event twice, once for forward propagation and once backwards, the backscatter level from the assembly through a loss event drops by two times the amount of loss. That is, for a 0.1 dB loss, the backscatter level drops 0.2 dB.

The same length of fiber was used leading up to each splice shown in Fig. 4. Note the repeatability in the scatter signature from the fiber leading up to the splices. This is typical of the Rayleigh scatter signature in optical fiber. Though we have not conducted extensive studies, it appears that this signature is permanent. That is, for a given length of fiber, the Rayleigh scatter signature is static over a very long period of time. This leads one to believe that this signature can actually be used to permanently identify certain important fiber lengths and locate them in a complex optical network. An early demonstration of this capability is given in reference 5.

We tested the insertion loss accuracy by measuring a nine pole optical switch using both the method described here and the more standard cut-back and splice method. The results are shown in Fig. 4. The top panel displays the measurement of the scatter level through the switch including connectors on both the input and output sides and the different lengths of fiber through the assembly. Figure 4 (b) shows a "blow up" of the switching section of the network. The individual interfaces within the switching mechanism are clearly resolved. The drop in the scatter internal to the switch is most likely due to sections of free space and other materials that don't scatter as strongly as fiber.

Using optical backscatter reflectometry, the insertion loss on either side of the switch is estimated by averaging the scattering signature over a certain length. For this example, the integration width was set to 0.25 m. The measured loss values are shown in Fig. 4 (c). The results using the backscatter reflectometer described here and the standard splicing method show agreement to within 0.1 dB.

It is worth noting that for the example of loss measurements through a switch, there is a substantial time savings when using the reflectometric technique. The reflectometric technique requires only one optical connection to measure the insertion loss of every channel of the switch; it requires only that the switch state is toggled to measure the loss through each port. This resulted in a total time of test of 4.5 minutes using backscatter reflectometry as compared to an average time of test of 20 minutes using the standard technique. The reflectometric technique has the further advantage of being able to measure the loss of the switch, in a single scan, both with and without the connectors. So, when accuracies of 0.1 dB are required, the reflectometric technique displays clear advantages over conventional techniques.

The last example is shown in Figure 5. This figure displays the reflectivity through a 1 dB tap coupler. One of the fibers on the output side of the coupler is "pinched" off very close to the coupler. The other fiber is about 8 meters long and a bad splice is clearly visible just after nine meters. In the inset of this figure is displayed an expansion of the coupling region. This coupler shows a signature that is typical of fused tapered couplers. In the taper region, the scatter level drops. We believe that this is caused by the mixing of the mode fields of the two coupled fibers and the transfer of power density from the core of the fiber to the cladding.

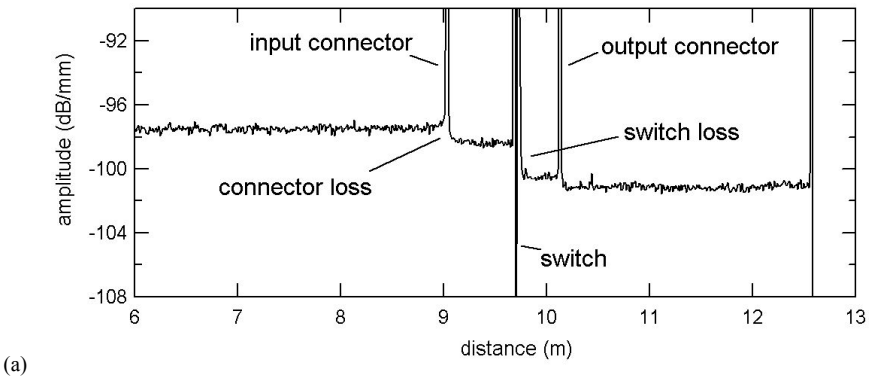

(a)

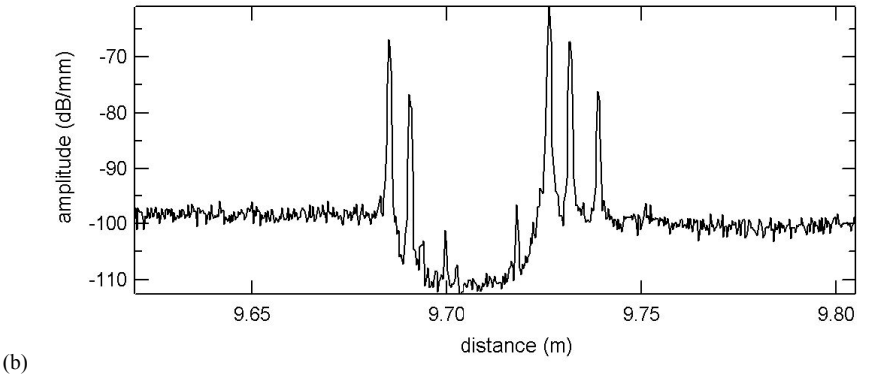

(b)

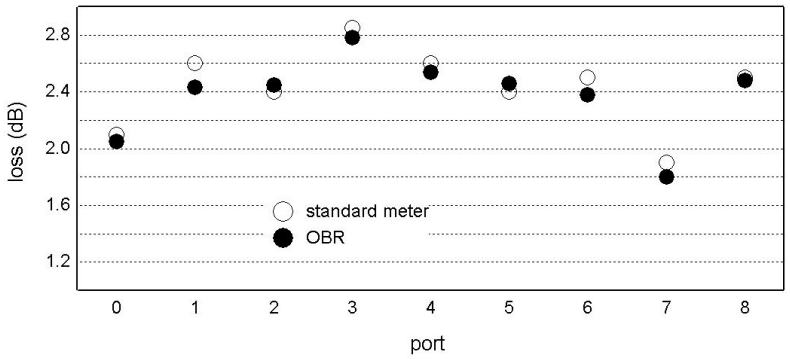

(c)

Fig. 4. (a) Reflection through one pole of a nine pole optical switch showing both input and output connectors and fiber, and the internal switching mechanism, (b) a high resolution of the switching mechanism, and (c) insertion loss data using optical backscatter reflectometry (OBR, black dots) and a power meter and splicing (white dots).

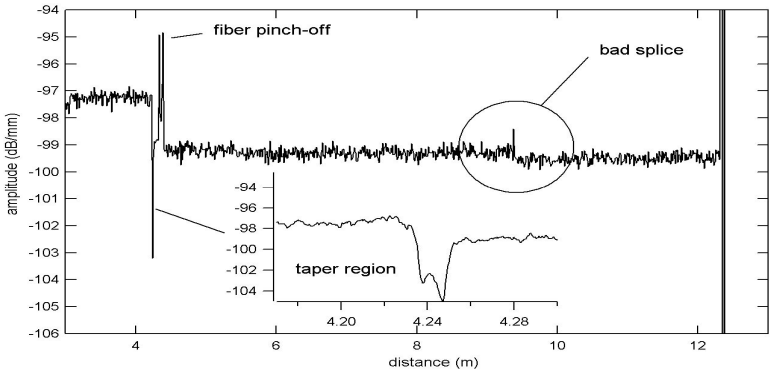

Fig. 5. Backscatter reflectivity through a 1 dB tap coupler with one output showing a bad splice.

5. Conclusions

We have demonstrated a method for polarization diverse measurements of Rayleigh backscatter in optical fiber and fiber-coupled components. With this method, we achieved 40 μm resolution measurements over 30 m of optical assembly length in a single scan of a tunable laser, the entire process taking only seconds. Sensitivities of greater than -125 dB were achieved by using a tunable laser with favorable phase noise characteristics, using quite amplification electronics and carefully choosing the receiver bandwidths. We observed a total dynamic range of just over 60 dB. That is, reflections in a test system stronger than -70 dB began to affect the level of the noise floor. Though 60 dB dynamic range is quite good, it is likely that this could be extended by the use of higher resolution DAQ electronics.

Careful calibration of the effects of the amplifiers on the backscatter signal as a function of length allows the system to be used as both a precise measurement tool for both return loss and insertion loss. Optical backscatter reflectometry not only allows one to locate reflective events in an assembly, but to also locate non-reflective insertion loss events such as bends and bad splices. Comparison with conventional techniques shows that the backscatter technique is capable of resolving insertion loss events of 0.05 dB and estimating the loss to within 0.1 dB. The backscatter technique has significant advantages in speed of test when compared to traditional techniques. Backscatter reflectometry also allows one to measure losses in a system independent of connectors.

While the system is polarization sensitive, the measurement results represent the response of the DUT to a single input polarization state. Polarization dependent losses can be measured by averaging data sets taken over a diversity of input polarization states. Investigations into the efficacy of this technique are underway.

The two channel polarization diversity detection gives this technique the ability to track changes in the polarization state of the light that propagates through the device or system under test. This unique and powerful feature allows one to identify locations within a device or assembly that have the great effect on the polarization state of the light. This is evident in the beating of the two dashed curves in Fig. 2. It should be noted that the polarization tracking is not accomplished by measuring the actual polarization state of the light as it propagates down an assembly. Polarization tracking is accomplished by monitoring the amplitude of the interference between the light reflected from the DUT and the two reference fields determined by the polarization beam splitter. However, the information provided by this method is quite useful nonetheless when faced with diagnosing polarization related issues in an assembly of components.

The technique presented here has distinct advantages in range, resolution, speed, accuracy, sensitivity and dynamic range for measurement applications from the component to the assembly level. Because it is based on the use of widely available tunable laser technology and relatively simple hardware, we believe that equipment based on this technique will prove to be indispensable to the process of building, testing and troubleshooting optical equipment.

References

[1] U. Glombitza and E. Brinkmeyer, "Optical frequency domain reflectometry for characterization of single-mode integrated optical waveguides," *J. Lightwave Tech.* **11**, 1377-1384 (1993).
[2] J. P. von der Weid, R. Passy, G. Mussi, and N. Gisin, "On the characterization of optical fiber network components with optical frequency domain reflectometry," *J. Lightwave Tech.* **15**, 1131-1141 (1997).
[3] J. P. von der Weid, R. Passy, and N. Gisin, "Coherent reflectometry of Optical Fiber Amplifiers," *IEEE Photon. Tech. Lett.* **9**, 1253-1255 (1997).
[4] M. Froggatt and J. Moore, "High resolution strain measurement in optical fiber with Rayleigh scatter," *Appl. Opt.* **37**, 1735-1740 (1998).
[5] M. Froggatt, B. Soller, D. Gifford, and M. Wolfe, "Correlation and keying of Rayleigh scatter for loss and temperature sensing in parallel optical networks," *OFC Technical Digest*, Los Angeles, March, 2004, paper PDP 17.
[6] B. Huttner, J. Reecht, N. Gisin, R. Passy, and J. P. von der Weid, "Local birefringence measurements in single-mode fibers with coherent optical frequency-domain reflectometry," *IEEE Photon. Tech. Lett.* **10**, 1458-1460 (1998).
[7] These operators denote the splitting of the input light by the beam splitter into two orthogonal polarizations denoted 's' and 'p'.